A Bayesian Neural Network-Based Method for the Extraction of a Metabolite Corrected Arterial Input Function from Dynamic [^{11}C]PBR28 PET

Alexander C. Whitehead* *Student Member, IEEE*, Ludovica Brusaferri*, Lucia Maccioni, Matteo Ferrante, Marianna Inglese, Zeynab Alshelh, Mattia Veronese, Nicola Toschi, Jodi Gilman, Kris Thielemans *Senior Member, IEEE*, and Marco L. Loggia

Abstract—In Positron Emission Tomography (PET), arterial sampling and metabolite correction are prerequisites for the gold-standard measurement of values like the volume of distribution (V_T), often necessary for the full quantification of radioligand binding. However, the invasiveness and technical demands of these procedures limit their application in both research and clinical PET studies. Machine learning approaches have been explored to predict V_T from PET images, but their integration in clinical routine is limited by their lack of transparency or thorough evaluation. Here we propose a Bayesian Neural Network to estimate the arterial input function (AIF), while also outputting its prediction uncertainty, 1) directly from the entire dynamic PET images (NN-AEIF), 2) from an image-derived input function (IDIF) (NN-IDIF) and, as a sensitivity measure, 3) from the un-corrected plasma curve (NN-AIF). All methods, applied on [^{11}C]PBR28 PET data, were compared to the metabolite-corrected AIF in terms of V_T, and the prediction uncertainty was assessed in terms of normalised coefficient of variance (nCV). Overall, both NN-AEIF and NN-AIF were able to accurately predict V_T, outperforming the other methods, with NN-AEIF showing the lowest nCV.

Index Terms—Arterial Input Function Estimation, Signal Extraction, Dynamic PET, Machine Learning, Bayesian Neural Networks

I. INTRODUCTION

THE Volume of Distribution (V_T) estimated with an Arterial Input Function (AIF) is utilised for quantification of many Positron Emission Tomography (PET) tracers, including [^{11}C]-Peripheral Benzodiazepine Receptor ([^{11}C]-PBR28). This, however, requires the concurrent measurement of the concentrations of unchanged radioligand in arterial plasma. Although insertion of an arterial catheter rarely results in clinically relevant adverse events, it is an invasive and laborious procedure.

Image Derived Input Function (IDIF) represents a promising alternative to arterial sampling [1]. However, its applicability in clinical research is hampered by several factors including the inaccuracy in the estimation of both shape and amplitude of the Input Function (IF); moreover IDIF does not allow for radio-metabolites quantification [2]. The application of Machine Learning (ML) is expected to improve the accuracy of predicting the AIF from PET images [3], [4]. While these methods have shown promising results, the vast majority of these approaches have been developed for PET tracers that do not produce radio-metabolites. Furthermore, even if the developed model shows sufficient prediction accuracy for unseen data, its applicability in the clinical setting remains questionable because of a lack of transparency or thorough evaluation [5]. Bayesian networks offer the significant advantage of making probabilistic predictions based on available evidence. Specifically, a Bayesian network would output uncertainty estimates in addition to the model prediction. For this reason, they have the potential to overcome the key barrier to the responsible adoption of Artificial Intelligence (AI) in clinical practice [6].

Here, we propose a Bayesian Neural Network (NN)-based method for predicting a metabolite corrected AIF, while allowing for the estimation of uncertainty of the model's output.

II. METHODS

A. Data Acquisition and Processing

Dynamic [^{11}C]-PBR28 PET/Magnetic Resonance (MR) images from 52 individuals (Age: 55 ± 16 years; Sex: 27 Male, 25 Female; Genotype: 32 High Affinity Binders (HABs), 20 Mixed Affinity Binders (MABs); Clinical population: 12 Healthy Controls, 40 Chronic Pain patients; Injected Dose: 14.16 ± 1.3 Millicuries (mCis)) were acquired on a Siemens Biograph mMR whole-body tomograph for a time-period of 0-90 minutes post-injection. Data were pooled for multiple protocols (approved by the Partners Healthcare/Mass General Brigham Institutional Review Board) and reconstructed as in [7]. All subjects had a radial artery catheter placed during the scan. Uncorrected plasma curves from blood samples were interpolated and metabolite-corrected to obtain the AIF. To further validate the proposed method, IDIF was calculated by segmenting the arterial carotid siphons using intensity thresholding of early dynamic PET frames. Data were split using ten-fold cross-validation, ensuring maximum within-variance and minimum between-variance in the training and testing sets.

B. Neural Network Design

The method is comprised of three independent NNs: NN_1 seeks to reduce the dimentionality of the input data (due to computational requirements) and extract the most relevant features. NN_2 aims to extract a non-metabolite corrected signal from the low-dimensional representation output by the first network. NN_3 metabolite corrects and reshapes/rescales the non-metabolite corrected signal.

1) NN_1 Autoencoder (AE): This network features three blocks, the downsampling block, the latent layer, and the upsampling block. The first block comprises three convolutions; the latent block is flanked on either side by two convolutions, with a variational latent layer in the middle. The upsampling block consists of a transposed convolution and two standard convolutions. Here, two downsampling and two upsampling blocks here used. The number of filters doubled or halved at each block respectively.

The input to the network is the dynamic PET images. Both the mean and standard deviation of the latent layer and the final layer are output from the model and passed onto NN_2. Both input and target data were standardised separately, based on parameters obtained from the training set. Each time frame was treated as an independent training example.

2) NN_2 Signal Extractor: This network consists of two blocks, the downsampling block and the fully connected block. The downsampling block follows the same structure as in NN_1. The fully connected block consists solely of one fully connected layer. All time frames were used simultaneously, where the same convolutions are applied independently on each time frame before global average pooling and flattening. After flattening the clinical features were concatenated with the flattened output. Here, four downsampling blocks and eight fully connected blocks were used. The number of filters doubled and the number of units halved at each block respectively.

3) NN_3 Metabolite Correction and Reshaping: This network contains solely fully connected layers. If the network is to metabolite-correct a signal (e.g. from AIF or IDIF), it takes that signal as input together with the clinical/demographic features (age, sex, genotype, injected dose, clinical population). If the network is instead to correct a signal obtained with NN_2, both the mean and the standard deviation of the uncorrected signal are input to NN_3, in addition to the latent layer from NN_2.

C. Evaluation

The model was sampled 32 times resulting in multiple realisations of the estimated signal. Then, $V_T \in \mathbb{R}^{r \times s \times b}$ were computed via the Logan graphical method, where r is the number of Region Of Interests (ROIs) ($r = 69$), s is the number of subjects ($s = 5$) and b is the number of model samples ($b = 32$). For both AIF and IDIF, $b = 1$. For the NN-based methods, V_T were computed for each model realisation and then used to calculate the mean V_T and its standard deviation. Moreover, the Normalised Coefficient of Variance (nCV) was defined as $\text{nCV} = \text{std}(Pred\ V_T)/True\ V_T$ with $\text{nCV} \in \mathbb{R}^{r \times s}$, where V_T is computed from the measured AIF. For each candidate signal, correlation analyses were performed on the V_T values (computed for all the ROIs and for all the subjects in the test-set) to the ones obtained with the ground truth signal (**TRUE-AIF**, see Section II-A). To measure the accuracy of the prediction, the angle between the regression- and the identity-line was also computed, defined as $\theta = 45 - \arctan(m) * 180/\pi$, with m being the slope of the regression-line. Furthermore, nCVs were averaged across ROIs for each subject of the test-set and compared via a paired t-test for each of the three NN-based methods.

Candidate Signals:

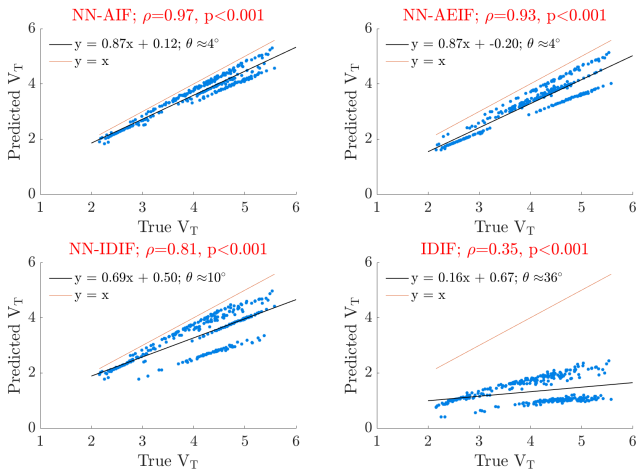- **IDIF** - generated as in Section II-A.

Fig. 1. Predicted $V_T \in \mathbb{R}^{r \times s}$ in the test-set subjects, with $r = 69$ and $s = 5$ estimated with the four candidate signals, correlated to the True V_T (obtained with TRUE-AIF). Please note that for the NN-based methods, the displayed V_Ts was averaged over all realisations.

- **NN-IDIF** - metabolite-corrected IF obtained from IDIF input to NN_3.
- **NN-AIF** - metabolite-corrected AIF obtained from (uncorrected) arterial plasma input to NN_3.
- **NN-AEIF** - metabolite-corrected IF obtained from dynamic PET images input to $NN_{1,2,3}$.

III. RESULTS

Fig. 1 reports the correlation analyses between the predicted V_T values (obtained by the four candidate methods) and the true V_T values. For all methods, predicted V_T values positively correlate with true V_T values, with NN-AIF and IDIF showing the highest and the lowest Pearson correlation coefficient (ρ), as well as the smallest and largest angular distance to the identity line, respectively: $\rho = 0.97$ & $\theta \approx 4°$ vs $\rho = 0.35$ & $\theta \approx 36°$. Overall, NN-AEIF outperformed NN-IDIF in terms of Pearson correlation coefficient and angular distance: $\rho = 0.93$ & $\theta \approx 4°$ vs $\rho = 0.81$ & $\theta \approx 10°$. With regard to the variance analysis, NN-AEIF outperforms both NN-AIF and NN-IDIF, showing the lowest nCV, while NN-AIF and NN-IDIF do not differ in terms of nCV values (p> 0.05).

IV. DISCUSSION AND CONCLUSION

This work presents an innovative Bayesian NN-based approach for estimating the AIF from dynamic PET images and clinical variables. This approach shares similarities with previous methods developed for PET tracers that do not produce radio-metabolites, such as [18F]fluorodeoxyglucose (FDG). In this study, additional efforts were devoted to address [11C]-PBR28 radio-metabolite correction. One of the main advantages of the proposed method is that it provides a measure of confidence in the generated signal for unseen data. Additionally, the method's modular design allows each part to be used independently. For example, in this work, metabolite correction was applied to a signal generated by a more traditional method (IDIF).

The four candidate signals were compared to the gold standard TRUE-AIF, obtained from arterial blood sampling and metabolite correction. Overall, NN-AEIF demonstrated comparable performance in terms of correlation and bias to NN-AIF, with the lowest variance of the estimated V_T, as measured by the nCV. This improved performance can potentially be explained by the larger amount of input data and the consequently more complex model with additional parameters. Interestingly, the NN-IDIF method was able to improve on the traditional IDIF approach, as evidenced by a higher correlation coefficient and a lower angular distance from the identity line.

The proposed approach has some limitations, including the small training size, which hindered the assessment of the prediction accuracy within subsets of clinical populations in the test-set (i.e., patients vs healthy controls). In the future, the accuracy of the model could be improved through the inclusion of an attention layer either before or after the latent layer of the AE, validated through the use of an ablation study. As well as the replacement of the fully connected layers with a transformer based approach.

REFERENCES

[1] P. Zanotti-Fregonara *et al.*, "Image-derived input function for brain PET studies: Many challenges and few opportunities," *Journal of Cerebral Blood Flow and Metabolism*, vol. 31, no. 10, pp. 1986–1998, 2011.

[2] H. Sari *et al.*, "Non-invasive kinetic modelling of PET tracers with radiometabolites using a constrained simultaneous estimation method: evaluation with 11C-SB201745," *EJNMMI Research*, vol. 8, 2018.

[3] S. Kuttner *et al.*, "Machine learning derived input-function in a dynamic 18F-FDG PET study of mice," *Biomedical Physics and Engineering Express*, vol. 6, no. 1, 2020.

[4] M. Ferrante *et al.*, "Physically Informed Neural Network for Non-Invasive Arterial Input Function Estimation In Dynamic PET Imaging," *Medical Imaging with Deep Learning – Under Review*, pp. 1–3, 2022.

[5] Z. Salahuddin *et al.*, "Transparency of deep neural networks for medical image analysis: A review of interpretability methods," *Computers in Biology and Medicine*, vol. 140, no. October 2021, p. 105 111, 2022.

[6] S. Prabhudesai *et al.*, "Lowering the computational barrier: Partially Bayesian neural networks for transparency in medical imaging AI," *Frontiers in Computer Science*, vol. 5, 2023.

[7] L. Brusaferri *et al.*, "The pandemic brain: Neuroinflammation in non-infected individuals during the COVID-19 pandemic," *Brain, Behavior, and Immunity*, vol. 102, no. February, pp. 89–97, 2022.